

New Optical Supramolecular Compound Constructed from a Polyoxometalate Cluster and an Organic Substrate

Yi-Ming Xie, Qi-Sheng Zhang, Zhen-Guo Zhao, Xiao-Yuan Wu, Shan-Ci Chen, and Can-Zhong Lu*

State Key Laboratory of Structural Chemistry, Fujian Institute of Research on the Structure of Matter, Chinese Academy of Sciences, Fuzhou, Fujian 35002, China

Received March 13, 2008

A new optical supramolecular compound constructed from a polyoxometalate cluster and an organic substrate $[(\text{H}_3\text{O})(\text{C}_{12}\text{H}_{10}\text{N}_3)_2(\text{PW}_{12}\text{O}_{40})]$ (1) has been synthesized via a hydrothermal reaction and has been structurally characterized by X-ray diffraction. The solid-state diffuse reflectance, IR, and photoluminescence spectra of the title compound indicate that there is an interaction between the α - $\text{PW}_{12}\text{O}_{40}$ and the organic substrate. The light-yellow title compound shows a certain second-order nonlinear optical response of $I^{\omega} = 2I_{\text{KDP}}^{\omega}$.

Introduction

Polyoxometalates (POMs), a large family of metal–oxygen clusters of the early transition metals in high oxidation states (most frequently W and Mo),¹ allow wide versatility in terms of shape, polarity, redox potential, surface charge distribution, and acidity because of their diversity in structure and composition.² In the past few years, there has been a rapidly growing number of reports in the literature that addresses the uses of POMs in catalysis and medicine.³ However, to our knowledge, only a handful of chiral compounds containing polyoxoanions have been featured in reports that discuss the photochemical and photochromism processes of POMs.⁴ Furthermore, there are few papers that involve the investigation of the nonlinear optical properties of this kind of compound, such

as nonlinear optical second harmonic generation (SHG).⁵ The study of nonlinear optical materials is very interesting and vigorous because of the wide use of this property.⁶ It has been reported that the electron donor–acceptor compound may serve as a potential high-efficiency second-order nonlinear optical material.⁷ It is widely recognized that POM acts as an electron acceptor and has the ability to be reduced and the organic substrate, 3-HPBIM, acts as a donor and has a large dipole moment and an unusually high basicity. In our former experiments, POM and 3-HPBIM, in principle, may form an incorporable compound with an asymmetrical element under solvothermal conditions, which might offer some novel optical properties. We report herein the synthesis, purification, crystal structure, photoluminescence, ESR, solid-state diffuse reflectance (DR), TG, and nonlinear optical properties of the discrete intermolecular compound composed of an organic substrate and a polyoxotungstate.

* To whom correspondence should be addressed. E-mail: czlu@fjirsm.ac.cn. Fax: (+86)-591-83705794.

- (1) *Polyoxometalate Chemistry: From Topology via Self-Assembly to Applications*; Pope, M. T., Müller, A., Eds.; Kluwer Academic: Dordrecht, The Netherlands, 2001, pp 315–417.
 (2) (a) Hill, C. L. *Chem. Rev.* **1998**, *98*, 1–2. (b) Murphy, D. W.; Christian, P. A. *Science* **1979**, *205*, 651–656. (c) Xu, B.; Peng, Z.; Wei, Y.; Powell, D. R. *Chem. Commun.* **2003**, 2562–2563.
 (3) (a) Judd, D. A.; Nettles, J. H.; Nevins, N.; Snyder, J. P.; Liotta, D. C.; Tang, J.; Ermolieff, J.; Schinazi, R. F.; Hill, C. L. *J. Am. Chem. Soc.* **2001**, *123*, 886–897. (b) Witvrouw, M.; Weigold, H.; Pannecouque, C.; Schols, D.; De Clercq, E.; Holan, G. *J. Med. Chem.* **2000**, *43*, 778–783. (c) Reinoso, S.; Vitoria, P.; Lezama, L.; Luque, A.; Gutiérrez-Zorrilla, J. M. *Inorg. Chem.* **2003**, *42*, 3709–3711. (d) Ma, B.-Q.; Zhang, D.-S.; Gao, S.; Jin, T.-Z.; Yan, C.-H.; Xu, G.-X. *Angew. Chem., Int. Ed.* **2000**, *39*, 3644–3646. (e) Rhule, J. T.; Hill, C. L.; Judd, D. A.; Schinazi, R. F. *Chem. Rev.* **1998**, *98*, 327–357. (f) Wang, X.-L.; Qin, C.; Wang, E.-B.; Su, Z.-M.; Hu, C.-W.; Xu, L. *Angew. Chem., Int. Ed.* **2004**, *43*, 5036–5040.

- (4) (a) Xin, F.; Pope, M. T. *J. Am. Chem. Soc.* **1996**, *118*, 7731–7736. (b) Sadakane, M.; Dickman, M. H.; Pope, M. T. *Inorg. Chem.* **2001**, *40*, 2715–2719. (c) An, H.; Xiao, D.; Wang, E.; Li, Y.; Xu, L. *New J. Chem.* **2005**, *29*, 667–672.
 (5) Zhang, X.-M.; Shan, B.-Z.; Duan, C.-Y.; You, X.-Z. *Chem. Commun.* **1997**, 1131–1132.
 (6) (a) Chen, C.; Liu, G. *Annu. Rev. Mater. Sci.* **1986**, *16*, 203–243. (b) Becker, P. *Adv. Mater.* **1998**, *10*, 979–992. (c) Chen, C.; Wang, Y.; Wu, B.; Wu, K.; Zeng, W.; Yu, L. *Nature* **1995**, *373*, 322–324. (d) Chen, C.; Wu, B.; Jiang, A.; You, G. *Sci. Sin., Ser. B* **1985**, *28*, 235–243. (e) Chen, C.; Wu, Y.; Jiang, A.; Wu, B.; You, G.; Li, R.; Lin, S. *J. Opt. Soc. Am. B* **1989**, *6*, 616–621.
 (7) Di Bella, S.; Fragala, I. L.; Ratner, M. A.; Marks, T. J. *J. Am. Chem. Soc.* **1993**, *115*, 682–686.

Experimental Section

Materials and Methods. The ligand 3-HPBIM [2-(3-pyridyl)-benzimidazolium] was prepared according to the literature methods.⁸ Other reagents and solvents were obtained from commercial sources and were used without further purification. Elemental analyses of carbon, hydrogen, and nitrogen were carried out on an Elementar vario EL. Infrared spectra were obtained by a Perkin-Elmer Spectrum One FT-IR spectrometer using KBr discs. The X-band ESR spectra were recorded on a Bruker 2000D-SRC spectrometer on powder crystal materials at 298 K. Thermal stability studies were carried out on a NETSCHZ STA-449C thermoanalyzer in an air atmosphere (30–1200 °C) at a heating rate of 10 °C·min⁻¹. The solid-state optical DR spectrum and the UV–visible absorption spectrum were measured at room temperature with a Perkin-Elmer Lambda 900 UV–visible spectrophotometer over a range of 190–3500 nm. A BaSO₄ plate was used as a standard (100% reflectance) for the measurement of the solid-state optical DR spectrum. The measurement of the powder frequency-doubling effect was carried out on the unsieved title compound powder by means of the method of Kurtz and Perry.⁹ The fundamental wavelength is 1064 nm and was generated by a Q-switched Nd:YAG laser. The SHG wavelength is 532 nm. KDP powder was used as a reference to assume the effect. A photoluminescence analysis was performed on an Edinburgh FLS920 fluorescence spectrometer.

Synthesis of [(H₃O)(C₁₂H₁₀N₃)₂(PW₁₂O₄₀)] (1). A mixture of H₃PW₁₂O₄₀ (1.44 g, 0.05 mmol), 3-HPBIM (0.10 g, 0.51 mmol), isophthalic acid (0.166 g, 1 mmol), methanol (5 mL), and H₂O (5 mL) was heated in a 23 mL Teflon-lined reaction vessel at 180 °C for 5 days. The autoclave was then cooled at 5 °C·h⁻¹ to room temperature. The light-yellow block crystals of the title compound were isolated, washed with water and ethanol, and dried at room temperature. Yield: 0.38 g (26.4% on the basis of W). Anal. Calcd for C₂₄H₂₃N₆O₄₁PW₁₂: H, 0.70; C, 8.76; N, 2.55. Found: H, 0.82; C, 8.63; N, 2.53.

Crystallographic Studies. The intensity data sets were collected on Siemens SMART CCD X-ray diffractometers with graphite-monochromated Mo K α radiation ($\lambda = 0.71073$ Å) by using an ω scan technique. Siemens SAINT software was used for data reduction and empirical absorption corrections.¹⁰ We solved the structures by direct methods by using the Siemens SHELXTL (version 5) crystallographic software package.¹¹ The difference Fourier maps based on these atomic positions yield the other non-hydrogen atoms. The hydrogen atoms, except for those on the lattice water molecules in which one of the two H atoms for each water molecule was generated from the difference Fourier maps, were generated theoretically, were allowed to ride on their respective parent atoms, and were included in the structure factor calculations with assigned isotropic thermal parameters, but they were not refined. We refined the structures by using a full-matrix least-squares refinement on F^2 . All atoms except for hydrogen atoms were refined anisotropically.

We measured powder X-ray diffraction (PXRD) patterns on a Rigaku DMAX2500 powder diffractometer at 40 kV and 100 mA

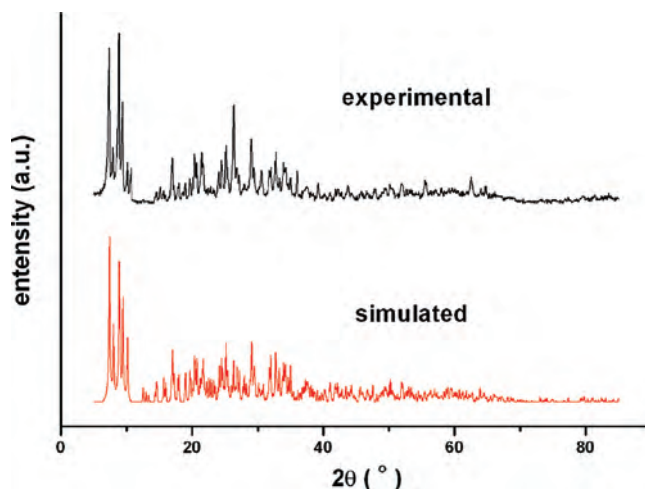


Figure 1. Experimental and simulated X-ray powder diffraction patterns of compound 1.

by using Cu K α radiation ($\lambda = 1.54056$ Å) with a scan speed of 0.375 s/step and a step size of 0.05°. The simulated powder patterns were calculated by our use of single-crystal X-ray diffraction data and were processed by the free Mercury (v1.4) program provided by the Cambridge Crystallographic Data Centre, as shown in Figure 1.

Results and Discussion

Syntheses. We prepared the title compound by exploiting the hydrothermal reactions of H₃PW₁₂O₄₀, 3-HPBIM, isophthalic acid, methanol, and H₂O at 180 °C for 5 days. The conditions reported in the Experimental Section are optimized for yields of crystalline products. Two key factors, the pH value and the isophthalic source, affect the formation of the resulting products. It is well known that the formation of different POM clusters is mainly controlled by the pH values. In our experiments, the best pH value was 2.1 for compound 1; at other pH values either no product could be obtained or the yields were very low. The selection of a suitable isophthalic source is the second key factor in our synthesis of the compound. Many failed former attempts in our experiments showed that the Keggin anions in the compound might readily act as charge-transfer supramolecules to produce an unchiral structure under hydrothermal conditions. A similar reaction without an isophthalic source leads to a symmetric structure. We speculated that the isophthalic source under hydrothermal conditions may play an important role in the formation of the chiral structure.

Description of Crystal Structure. Single-crystal X-ray crystallographic analysis reveals that compound 1's crystal structure is developed from an asymmetric unit composed of four independent components. Two HPBIM cations, one [H₃O]⁺ cation, and one [PW₁₂O₄₀]³⁻ anion lead to the molecular formula [(H₃O)(C₁₂H₁₀N₃)₂(PW₁₂O₄₀)] (1). The charge balance of the molecular formula requires the presence of three protons. However, these protons and the hydrogen atoms of the water molecules were generated geometrically (C–H bond fixed at 0.96, O–H at 0.85, and N–H at 0.86 Å) and were treated as riding. All non-hydrogen atoms were treated anisotropically. A summary of the crystallographic data is given in Table 1.

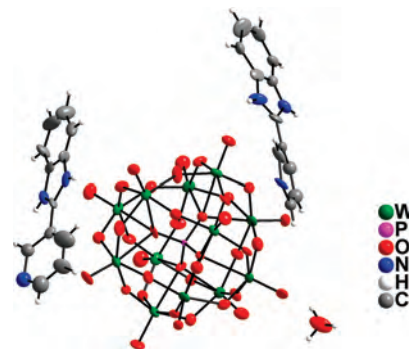
- (8) (a) Alcalde, E.; Dinarés, I.; Pérez-García, L.; Roca, T. *Synthesis* **1992**, 395–398. (b) Bauer, V. J.; Wiegand, G. E.; Fanshawe, W. J.; Safir, S. R. *J. Med. Chem.* **1969**, *12*, 944–945.
- (9) Kurtz, S. K.; Perry, T. T. *J. Appl. Phys.* **1968**, *39*, 3798–3813.
- (10) (a) *CrystalClear*, version 1.35; Molecular Structure Corp.: The Woodlands, TX, and Rigaku Corp: Tokyo, Japan, 2002. (b) *SAINT Software Reference Manual*; Siemens Energy & Automation Inc.: Madison, WI, 1994.
- (11) *SHELXTL Reference Manual*, version 5; Siemens Energy & Automation Inc.: Madison, WI, 1994.

Table 1. Crystal Parameters for **1**

formula	C ₂₄ H ₂₃ N ₆ O ₄₁ PW ₁₂
fw	3288.65
color	light yellow
cryst size (mm ³)	0.10 × 0.06 × 0.05
cryst syst	monoclinic
space group	P2 ₁
<i>a</i> (Å)	13.053(2)
<i>b</i> (Å)	17.422(4)
<i>c</i> (Å)	13.282(2)
β (deg)	114.184(2)
<i>V</i> (Å ³)	2755.3(8)
<i>Z</i>	2
2 θ _{max} (deg)	50.7
reflins collected	18 222
independent, obsd reflns (<i>R</i> _{int})	7945, 7017 (0.0776)
<i>d</i> _{calcd} (g/cm ³)	3.964
μ (mm ⁻¹)	25.068
<i>T</i> (K)	293(2)
<i>F</i> (000)	2880
<i>R</i> ₁ , w <i>R</i> ₂	0.0497, 0.1150
<i>S</i>	1.042
largest and mean Δ/σ	0.064, 0.003
$\Delta\rho$ (max/min) (e/Å ³)	4.454/(-2.395)

The view of the asymmetric unit presented in Figure 2 shows that the solvent molecules together with HPBIM bases surround the PW₁₂O₄₀ anion. The W–O bond distance of POM is in the range of 1.64–1.72 Å for the terminal oxygen, 1.87–1.97 Å for the bridging oxygen, and 2.40–2.48 Å for the oxygen of the PO₄ group. The P–O bond distances are 1.50, 1.54, 1.55, and 1.55 Å, respectively. The shortest W–O distance in the anion, W(12)–O(40), is 1.64 Å, and the longest W–O bond, W(3)–O(37), is 2.48 Å, which shows that the WO₆ octahedron of the anion is severely distorted (Table 2). The molecular packing diagram is shown in Figure 3. There are two types of hydrogen bonds between the polyanion and organic cation: N2–H2B···O17 (2.964(5)Å) and C–H···O (2.990(5)–3.198(5)Å) (Table 3). The pattern of the described hydrogen bonds leads to the formation of the layer structure (Figure S2). This means that there is certain interaction between the polyanion and the organic substrate that leads to a partial charge.¹² Most importantly, such intense hydrogen bond interactions between the N or C of organic cations and the polyanion changed the bond lengths and bond angles of the polyanion framework and therefore twisted the symmetric structure of α -Keggin POM, resulting in an unsymmetrical structure for **1**.

Ultraviolet–Visible Absorption Spectra. Diffuse reflectance (DR) spectra of the prepared compound were between 190 and 3500 nm and presented only one asymmetric band centered at ca. 350–360 nm. This band is mainly due to the presence of H₃PW₁₂O₄₀, whose DR spectra also have one band with λ_{max} near 350 nm. A pronounced tailing of this band into the visible region was observed for the title compound with significant absorption at $\lambda > 460$ nm and λ_0 (the value at which the absorbance reaches the baseline value) = 600 nm (Figure 4). In contrast, 3-PBIM and the corresponding heteropolyacids are transparent at $\lambda > 430$ nm. These results indicate intense charge transfer between

**Figure 2.** Molecular structure of compound **1**.**Table 2.** Selected Bond Lengths (Angstroms)

W(1)–O(3)	1.687(3)	W(7)–O(25)	1.910(3)
W(1)–O(18)	1.893(2)	W(7)–O(20)	1.925(3)
W(1)–O(6)	1.911(2)	W(7)–O(29)	1.943(3)
W(1)–O(33)	1.917(3)	W(7)–O(31)	2.430(3)
W(1)–O(27)	1.936(3)	W(8)–O(17)	1.719(3)
W(1)–O(37)	2.451(3)	W(8)–O(27)	1.872(3)
W(2)–O(39)	1.695(3)	W(8)–O(25)	1.883(2)
W(2)–O(8)	1.876(3)	W(8)–O(16)	1.895(3)
W(2)–O(23)	1.892(2)	W(8)–O(35)	1.911(2)
W(2)–O(20)	1.897(2)	W(8)–O(37)	2.439(3)
W(2)–O(16)	1.925(3)	W(9)–O(21)	1.657(4)
W(2)–O(30)	2.422(3)	W(9)–O(1)	1.867(3)
W(3)–O(15)	1.685(2)	W(9)–O(32)	1.902(2)
W(3)–O(11)	1.862(3)	W(9)–O(2)	1.915(3)
W(3)–O(38)	1.901(4)	W(9)–O(26)	1.919(3)
W(3)–O(18)	1.925(3)	W(9)–O(28)	2.435(3)
W(3)–O(35)	1.939(3)	W(10)–O(7)	1.697(3)
W(3)–O(37)	2.479(2)	W(10)–O(29)	1.887(3)
W(4)–O(12)	1.648(3)	W(10)–O(26)	1.907(3)
W(4)–O(23)	1.915(3)	W(10)–O(9)	1.912(3)
W(4)–O(19)	1.926(3)	W(10)–O(4)	1.930(3)
W(4)–O(5)	1.947(3)	W(10)–O(31)	2.408(2)
W(4)–O(11)	1.955(3)	W(11)–O(10)	1.652(3)
W(4)–O(30)	2.428(2)	W(11)–O(6)	1.881(3)
W(5)–O(36)	1.666(2)	W(11)–O(4)	1.887(3)
W(5)–O(5)	1.892(3)	W(11)–O(34)	1.900(3)
W(5)–O(38)	1.917(4)	W(11)–O(22)	1.967(3)
W(5)–O(14)	1.916(3)	W(11)–O(31)	2.459(3)
W(5)–O(32)	1.920(3)	W(12)–O(40)	1.636(4)
W(5)–O(28)	2.458(2)	W(12)–O(19)	1.882(2)
W(6)–O(14)	1.896(2)	W(12)–O(9)	1.885(3)
W(6)–O(34)	1.913(2)	W(12)–O(2)	1.890(3)
W(6)–O(1)	1.943(3)	W(12)–O(8)	1.973(3)
W(6)–O(28)	2.399(3)	W(12)–O(30)	2.441(3)
W(6)–O(13)	1.706(4)	P(1)–O(37)	1.504(3)
W(6)–O(33)	1.882(3)	P(1)–O(31)	1.539(2)
W(7)–O(24)	1.705(3)	P(1)–O(30)	1.549(3)
W(7)–O(22)	1.881(3)	P(1)–O(28)	1.551(3)

3-PBIM (probably as electron donor) and the PW₁₂ anions (electron acceptors) in the solids of compound **1**.¹⁴ However, the maxima of the charge-transfer bands cannot be indicated because only a broad envelope is observed (Figure 4). The red shift of λ_0 accompanied the increase in the reduction potential of the acceptor anions. This charge-transfer character is also confirmed by the crystal color change (H₃[PW₁₂O₄₀]·xH₂O, white → **1**, yellow), as observed for other charge-transfer salts.^{13,14} In the case of compound **1**, the asymmetry of the band at 350 nm and the absorption at

(13) Zhai, Q.-G.; Wu, X.-Y.; Chen, S.-M.; Zhao, Z.-G.; Lu, C.-Z. *Inorg. Chem.* **2007**, *46*, 5046–5058.

(14) (a) Le Maguerès, P.; Hubig, S. M.; Lindeman, S. V.; Veya, P.; Kochi, J. K. *J. Am. Chem. Soc.* **2000**, *122*, 10073–10082. (b) Niu, J.-Y.; Wei, M.-L.; Wang, J.-P.; Dang, D.-B. *Eur. J. Inorg. Chem.* **2004**, 160–170.

(12) Gamelas, J. A. F.; Santos, F. M.; Felix, V.; Cavaleiro, A. M. V.; de Matos Gomes, E.; Belsley, M.; Drew, M. G. B. *Dalton Trans.* **2006**, 1197–1203.

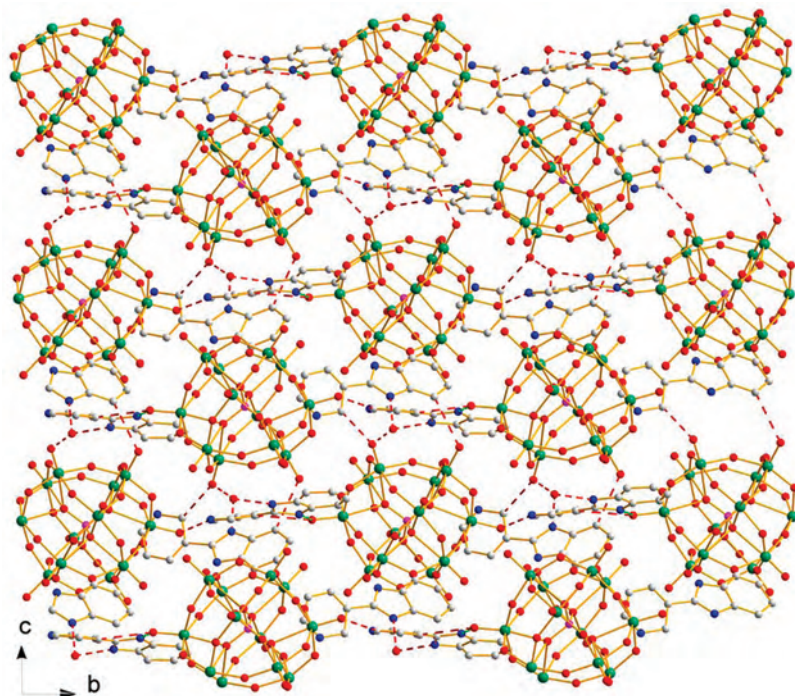


Figure 3. Packing diagram of compound **1** with dashed lines representing hydrogen bonds.

Table 3. Hydrogen Bond Lengths (Angstroms) and Bond Angles (deg) in Compound **1**^a

D–H···A	D–H	H···A	D···A	<(DHA)
N5–H5A···O1W ^b	0.86	1.90	2.760(5)	174.5
N2–H2B···O17 ^c	0.86	2.15	2.964(5)	158.6
N1–H1B···O1W ^d	0.86	1.83	2.682(5)	170.3
O1W–H1WC···O15	0.85	2.59	3.164(4)	126.0
C9–H9A···O17 ^c	0.93	2.27	3.150(6)	158.7
C11–H11A···O21 ^e	0.93	2.31	3.198(5)	158.5
C13–H13A···O36 ^b	0.93	2.61	3.160(4)	118.6
C21–H21A···O15 ^b	0.93	2.28	2.990(5)	133.2
C23–H23A···O4 ^f	0.93	2.59	3.113(6)	115.8

^a Symmetry transformations used to generate the equivalent atoms. ^b ($x - 1$), y , ($z - 1$). ^c ($-x + 1$), ($y + 1/2$), ($-z + 2$). ^d ($x - 1$), y , z . ^e ($-x + 1$), ($y - 1/2$), ($-z + 2$). ^f ($-x$), ($y - 1/2$), ($z + 1$).

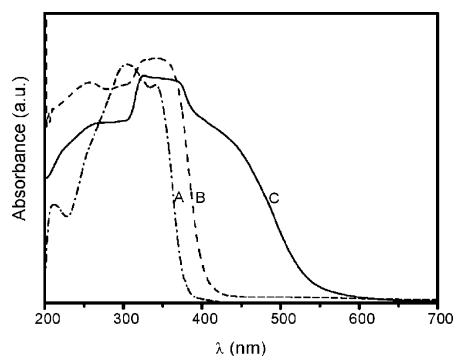


Figure 4. UV–visible absorption spectra of (A) 3-HPBIM, (B) $\text{H}_3\text{PW}_{12}\text{O}_{40}$, and (C) compound **1**.

$\lambda > 460$ nm may also indicate a charge-transfer interaction of the organic and inorganic entities (Figure 4).

Photoluminescence Properties. The emission spectra of the compound and the free 3-PBIM ligand in solid state at room temperature are shown (Figure 5). The excitation of the solid sample **1** at $\lambda = 340$ nm produces intense blue luminescence with a peak maximum at 429 nm. To understand the nature of the emission bands, we analyzed the

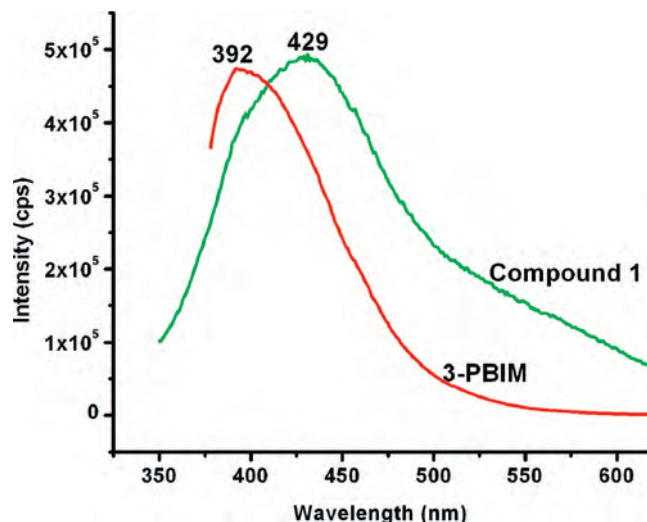


Figure 5. Emission spectra of 3-PBIM and **1** in the solid state at room temperature.

photoluminescence property of the 3-PBIM ligand and found that the emission peak for 3-PBIM is at 392 nm. The intense emission peak for **1** may be tentatively assigned to the intraligand transition of the free ligand's fluorescence emissions.¹⁵

Fourier Transform Infrared Spectra, Electron Spin Resonance, and Thermogravimetric Analyses. In the IR spectrum of compound **1** (Figure S1), the features at 1079, 978, 892, and 803 cm^{-1} are attributed to $\nu(\text{W}-\text{O}_t)$, $\nu(\text{W}-\text{O}_b)$, and $\nu(\text{W}-\text{O}_c)$ of the $[\text{PW}_{12}\text{O}_{40}]^{3-}$ anion. The peaks at 1639, 1469, 1419, 1319, and 1283 cm^{-1} are regarded as characteristic bands of the 2-(3-pyridyl)-benzimidazolium molecule. The peak positions that correspond to the Keggin anions

(15) Chen, L.-J.; He, X.; Xia, C.-K.; Zhang, Q.-Z.; Chen, J.-T.; Yang, W.-B.; Lu, C.-Z. *Cryst. Growth Des.* **2006**, *6*, 2076–2085.

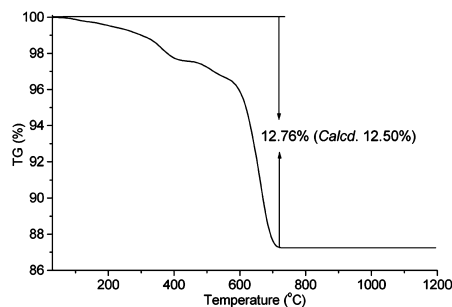


Figure 6. Thermogravimetric diagram of compound **1**.

slightly differ from those of the original acids, as can be observed for other transition-metal coordination fragments and Keggin ions or for organic–inorganic hybrids containing charge-compensating organics.¹³ The ESR spectra for the title compound are recorded on polycrystalline samples at room temperature (Figure S3). The result shows that the spectra of the compound are assigned to the intervalence charge-transfer IVCT band of $[\text{PW}_{12}\text{O}_{40}]^{3-}$, which indicates that electron transfer occurs between the organic substate and the POM cluster.^{16,17} The parameters $g_{\perp} = 1.9293$ and $g_{\parallel} = 1.9080$ are obtained for **1**. The thermal stability of compound **1** was investigated on a crystalline sample in an air atmosphere of 30–1200 °C. The TG curve of the title compound shows an obvious weight loss of 12.76% from 30 to 720 °C, which is attributed to the loss of guest water molecules and two HPBIM cations (calcd 12.50%). After this, no weight loss is found until 1200 °C, which indicates that the remaining $\text{PW}_{12}\text{O}_{40}$ anions do not decompose at temperatures up to 1200 °C. (Figure 6).

Nonlinear Optical Properties. The noncentrosymmetric structure of **1** prompts us to measure its SHG properties. The SHG measurements of the powder samples reveal that compound **1** exhibits a SHG efficiency of about 2 times that of KDP (KH_2PO_4), which is larger than that of the compound of $\text{H}_4\text{SiW}_{12}\text{O}_{40} \cdot 4\text{HMPA} \cdot 2\text{H}_2\text{O}$ ¹⁷ and $[4\text{-DMSP}]_4[\text{NH}_2\text{Me}_2]_2\text{-HSiFeMo}_{11}\text{O}_{40} \cdot 3\text{H}_2\text{O}$.⁵ Further absorption spectrum measurements indicate that compound **1** is transparent in the

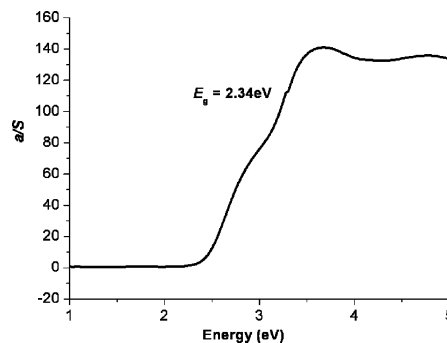


Figure 7. Diffuse reflectance spectrum of compound **1**.

range of 600–2000 nm. From 600 to 350 nm, the absorption increases with decreasing wavelength, and the largest absorption rate is ca. 27% at 350 nm (Figure 4). Hence compound **1** might be used in UV and near-IR regions as an NLO material. An optical DR study of compound **1** reveals that it is a semiconductor with a band gap of 2.34 eV (Figure 7), which is much smaller than the band gaps of the well-known and the best-used NLO crystals BBO (6.43 eV) and LBO (7.78 eV).¹⁸

Conclusions

The combination of the POM cluster and the organic substrate resulted in compound **1**, which has good SHG properties. Our future efforts will be devoted to the growth of large crystals and related physical property studies for this compound. We will also explore similar systems to find new NLO materials based on POMs.

Acknowledgment. This work was supported by the 973 Key Program of the MOST (2006CB932904, 2007CB815304, 2007CB815300), the National Natural Science Foundation of China (20425313, 20521101), the Chinese Academy of Sciences (KJCX2-YW-MO5), and the Natural Science Foundation of Fujian Province (2006F3135).

Supporting Information Available: Crystal data for **1**, FI-IR spectra for 3-HPBIM ligand and **1**, layer diagram of **1**, and ESR spectrum of **1**. This material is available free of charge via the Internet at <http://pubs.acs.org>.

IC800827A

(16) (a) Yamase, T. *Chem. Rev.* **1998**, *98*, 307–324. (b) Jeannin, Y.; Launay, J.-P.; Livage, J.; Nel, A. *Inorg. Chem.* **1978**, *17*, 374–377.

(17) Niu, J.-Y.; You, X.-Z.; Duan, C.-Y. *Inorg. Chem.* **1996**, *35*, 4211–4217.

(18) French, R. H.; Ling, J.-W.; Ohuchi, F. S.; Chen, C. T. *Phys. Rev. B* **1991**, *44*, 8496–8502.